

Suction Vortices, Spiral Breakdown and Multiple Vortices in Tornadoes

Brian Fiedler *

University of Oklahoma, Norman, Oklahoma

1. Introduction

Three-dimensional simulations of idealized, laminar, tornadic vortices under a perpetual buoyancy updraft were presented in Fiedler (1998). These simulations are being updated with modern computing power. Simulations at twice the resolution used in 1998 now reveal intense suction vortices capped by a spiral vortex breakdown. Though the spiral breakdown has commonly been studied in an engineering context (Lim and Cui 2003; Serre and Bon-toux 2002), those studies have not been focused on its role in maintaining, or limiting, the strong winds at the base of a tornado. That role is the focus in the current study. These simulations do not employ parameterized turbulence, as in Xia et al. (2003).

As these simulations move to higher Reynolds number the 1998 conclusion is still valid: "These results are exactly in line with the deduction of Fujita (1971), who estimated that a suction vortex would have a wind speed twice that of the parent vortex."

2. The Model

The numerical simulations are configured similar to those in Fiedler (1998). The numerical model is dimensionless. The domain is a box $4 \times 4 \times 1$ with a permanent central buoyancy field that, acting alone, would accelerate a parcel to one unit of velocity along the central axis of the model. Alternatively, the central buoyancy field could support a hydrostatic pressure deficit of one-half unit at the surface, with a wind speed of one unit in a surrounding stagnant-core potential vortex.

The grid has $181 \times 181 \times 91$ grid points. The grid is greatly stretched in both the vertical and horizontal. At the surface, the horizontal grid widths Δx and Δy are less than 0.0054 in the region $-.2 < x < .2$ and $-.2 < y < .2$, where the tornado forms. The grid is stretched in the vertical to enhance the resolution in the viscous boundary layer, leaving $\Delta z = 0.0022$ at the lowest level. The model has fifth-order, upwind-biased advection and an iterative solver to maintain

a close approximation to incompressibility.

The dimensionless viscosity ν is a constant ν_0 below $z = 0.5$ (for most cases $\nu_0 = .0001$). Above $z = 0.5$, ν increases linearly to 0.001 at the top boundary at $z = 1$. The lower boundary is no-slip, the other boundaries are free-slip (unless otherwise stated). A dimensionless Coriolis parameter f is the source of the vertical relative vorticity. In the simulations shown here, f varies from 0.07 to 0.15.

3. The Simulations

Figure 1 shows a time history of maxima quantities associated with the central vortex. The particular simulation has $\nu_0 = .0001$ and $f = 0.1$. Plotting pressure deficit as the equivalent speed q allows it to be conveniently plotted with wind speeds. Also, the degree to which the the pressure deficit is a dynamic pressure deficit can be assessed by comparing q with U . Such a comparison strictly requires that q and U be sampling the same point, which is usually the case. The fact that U is generally less than q shows that either some dissipation has occurred in the flow or that transient effects are substantial.

Figure 2 shows snapshots in four different simulations, within a rather narrow range of the parameter space. The viscosity is selected to be low enough to allow for suction vortices with a spiral vortex breakdown, but not so low as to lose confidence in the resolution provided by the grid. The swirl is selected to be large enough to allow for intense vortices, and to show the transition between single and multiple vortices. Larger values of swirl are not shown, because a larger parent vortex occurs, which tends to place the suction vortices outside the region of high resolution.

The transition to multiple vortices occurs with either increasing swirl f or decreasing viscosity ν_0 . Either course provides a viscous boundary layer that is too thin to turn into the vertical and to provide the core of a single, central vortex with a central updraft that would be compatible with the available pressure deficit.

12characters.net provides animations of the cases depicted in Fig. 2. From those animations,

* Corresponding author address: Dr. Brian Fiedler, School of Meteorology, 120 David L. Boren Blvd., Suite 5900, Norman, OK 73072; e-mail: bfiedler@ou.edu.

the following conclusions can be substantiated. For $\nu_0 = .0001$, as f increases from .07 to 0.1 to 0.15, we find (a) a single central vortex capped by a spiral breakdown, (b) occasional twin vortices, but usually at most one intense vortex orbiting in the parent vortex and (c) frequent twin vortices, both of which can be intense. A similar progression to multiple vortices in laboratory simulation is documented in Church et al. (1979). To what extent those multiple vortices were suction vortices is unknown; the pressure and velocity in the individual vortices were difficult to measure (Baker and Church 1979).

Figure 3 (bottom) shows a still image capture from a recent HD video taken by storm chasers Reed Timmer and Joel Taylor. The combination of close vantage point and absence of obscuring dust provided an exceptional record of suction vortices indicated by condensation. However, a view of the point of contact with the surface is apparently obscured by a slight dip in the terrain. Because the visualization is provided by condensation rather than dust, the low pressure of the suction vortices can be clearly inferred.

Though the suction vortices in Fig. 3 are multiple, this tornado would *not* be regarded as a multiple-vortex tornado. There is a hint of a suction vortex at the base of the top photo in Fig. 3. But only the most intrepid storm chasers could provide witness for this multiple suction vortex phenomenon that is seen at close approach. The multiple vortex phenomenon studied in Church et al. (1979) could be a distinctly larger scale phenomenon.

4. Conclusions

As already shown in Fiedler (1998), the presence of friction at the lower boundary allows transient suction vortices that orbit within a parent tornado. These suction vortices beat the *thermodynamic speed limit* of 1.0, the limit imposed by buoyancy of the core. The suction vortices routinely achieve a wind speed greater than 2.0.

The spiral structure and transient nature of the simulated vortices is very similar to those recently photographed in the Ellis County tornado. Likewise the simulated vortices behave as what Fujita (1971) has described suction vortices to be: explosive in development and often lasting less than one rotation of the parent vortex. Despite the idealized configuration of these simulations (in particular, their laminar nature), the simulations may be capturing the essence of suction vortex dynamics.

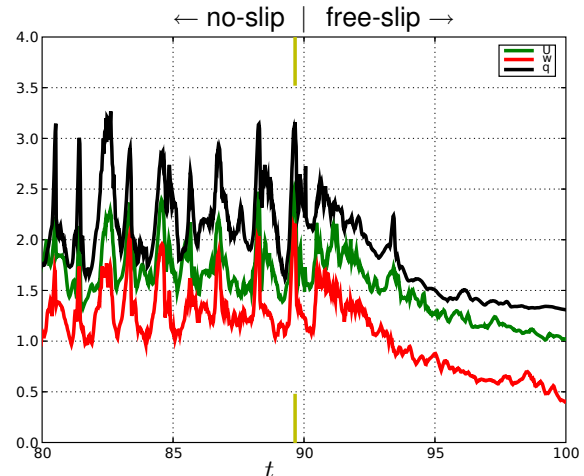


Figure 1: Time histories of the maxima in the domain for the last 20 time units with $\nu_0 = .0001$ and $f = .1$. w is the vertical component of velocity and U is the wind speed. Also shown is the minimum pressure fluctuation over density, denoted p , plotted as $q \equiv (-2p)^{\frac{1}{2}}$. At time $t = 90$ the lower boundary is converted to free slip. Wind speeds subsequently diminish as suction vortices dissipate. The light-green mark at $t = 89.66$ indicates the time depicted in Fig. 2.b and Fig. 4.

References

- Baker, G. L. and C. R. Church, 1979: Measurements of core radii and peak velocities in modeled atmospheric vortices. *J. Atmos. Sci.*, **36**, 2413–2424.
- Church, C. R., J. T. Snow, G. L. Baker, and E. M. Agee, 1979: Characteristics of tornado-like vortices as a function of swirl ratio: a laboratory investigation. *J. Atmos. Sci.*, **36**, 1755–1776.
- Fiedler, B. H., 1998: Wind-speed limits in numerically simulated tornadoes with suction vortices. *Q. J. R. Meteorol. Soc.*, **124**, 2377–2392.
- Fujita, T. T., 1971: Proposed mechanism of suction spots accompanied by tornadoes. *Preprints, Seventh Conf. Severe Local Storms*, Boston, 208–213.
- Lim, T. T. and Y. D. Cui, 2003: On the generation of a spiral-type vortex breakdown in an enclosed cylindrical container. *Phys. Fluids*, **17**, 044105.
- Serre, E. and P. Bontoux, 2002: Vortex breakdown in a three-dimensional swirling flow. *J. Fluid Mech.*, **459**, 347–370.

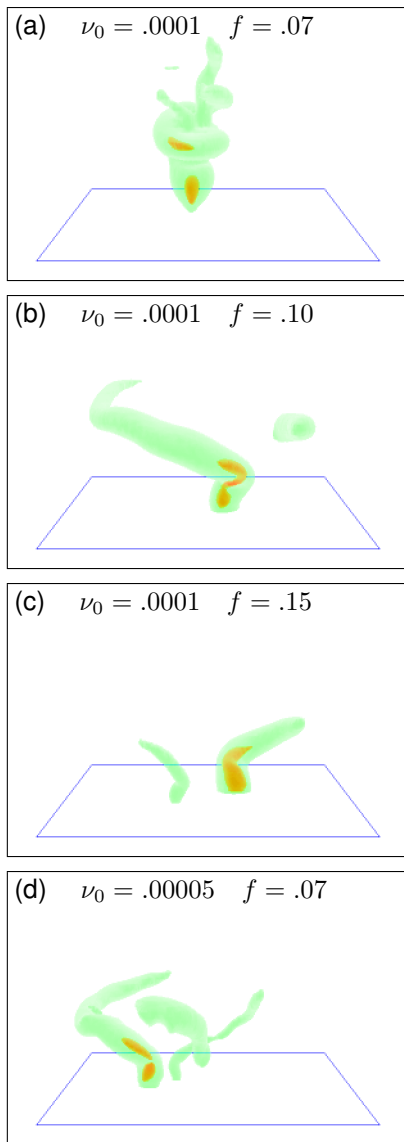


Figure 2: Snapshot of pressure isosurfaces of $p = -1$ (green) and $p = -2$ (red) at times of intense suction vortices in four different simulations, with the indicated values of ν_0 and f . The square at the lower boundary contains $-0.2 < x < 0.2$ and $-0.2 < y < 0.2$. More details can be found at 12characters.net.



Figure 3: Ellis County, OK tornado of May 4, 2007. Photos courtesy of Reed Timmer and Joel Taylor of TornadoVideos.net. Top image is from approximately 1 km away, a few minutes before the viewing at approximately 100 meters in the bottom image, in which suction vortices are evident at the base of the condensation funnel.

Xia, J., W. S. Lewellen, and D. C. Lewellen, 2003:
Influence of Mach number on tornado corner flow
dynamics. *J. Atmos. Sci.*, **60**, 2820–2825.

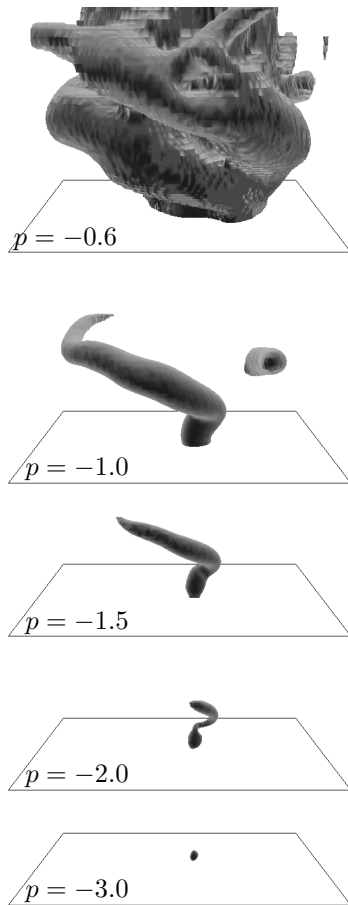


Figure 4: Five pressure isosurfaces for the intense event at $t = 89.66$ that is shown in Fig. 2.b.